JOURNAL OF VIROLOGY, Sept. 2005, p. 11693–11704 Vol. 79, No. 18
0022-538X/05/$08.00+0 doi:10.1128/JVI.79.18.11693–11704.2005

In-Depth Analysis of a Heterosexually Acquired Human Immunodeficiency Virus Type 1 Superinfection: Evolution, Temporal Fluctuation, and Intercompartment Dynamics from the Seronegative Window Period through 30 Months Postinfection†

F. E. McCutchan,[1]* M. Hoelscher,[2] S. Tovanabutra,[1] S. Piyasirisilp,[1] E. Sanders-Buell,[1] G. Ramos,[1] L. Jagodzinski,[1] V. Polonis,[1] L. Maboko,[3] D. Mmbando,[4] O. Hoffmann,[2,5] G. Riedner,[5] F. von Sonnenburg,[2] M. Robb,[1] and D. L. Birx[1]

U.S. Military HIV Research Program, 1600 E. Gude Drive, Rockville, Maryland 20850[1]; Department of Infectious Diseases and Tropical Medicine, Ludwig-Maximilians-University, Leopoldstrasse 5, Munich, Germany[2]; Mbeya Medical Research Programme, Mbeya, Tanzania[3]; Mbeya Regional Medical Office, Ministry of Health, Mbeya, Tanzania[4]; and London School of Hygiene and Tropical Medicine, 50 Bedford Square, London WC1B 3DP, United Kingdom[5]

Received 26 January 2005/Accepted 18 June 2005

Human immunodeficiency virus type 1 (HIV-1) superinfection refers to the acquisition of another strain by an already infected individual. Here we report a comprehensive genetic analysis of an HIV-1 superinfection acquired heterosexually. The infected individual was in a high-risk cohort in Tanzania, was exposed to multiple subtypes, and was systematically evaluated every 3 months with a fluorescent multiregion genotyping assay. The subject was identified in the window period and was first infected with a complex ACD recombinant strain, became superinfected 6 to 9 months later with an AC recombinant, and was monitored for >2.5 years. The plasma viral load exceeded 400,000 copies/ml during the first 9 months of infection but resolved to the set point of 67,000 copies/ml by 3 months after superinfection; the CD4 cell count was 377 cells/μl at 30 months. Viral diversity was evaluated with techniques designed to fully sample the quasispecies, permitting direct observation of the evolution, temporal fluctuation, and intercompartment dynamics of the initial and superinfecting strains and recombinants derived from them. Within 3 months of superinfection, seven different molecular forms were detected in *gag* and six were detected in *env*. The proportions of forms fluctuated widely over time in plasma and peripheral blood mononuclear cells, illustrating how challenging the detection of dually infected individuals can be. Strain-specific nested PCR confirmed that the superinfecting strain was not present until the 9 month follow-up. This study further defines the parameters and dynamics of superinfection and will foster appropriate studies and approaches to gain a more complete understanding of risk factors for superinfection and its impact on clinical progression, epidemiology, and vaccine design.

At every replication cycle, human immunodeficiency virus type 1 (HIV-1) recombines the two genomic RNA molecules packaged in the virion through the mechanism of strand switching at reverse transcription (7, 19). HIV-1-infected cells harbor, on average, four separate proviruses, whose genomic RNA transcripts have the opportunity to assort at the packaging stage and are recombined during the next replication cycle (21). Recombination reshuffles point mutations arising in the infected individual (40) but gains new significance when individuals become infected with more than one HIV-1 strain, either from the same or from different subtypes. In this case, recombination provides for a series of adjacent mutations to be acquired (or discarded) simultaneously (36). Intersubtype recombinant HIV-1 strains, which are easier to detect than their intrasubtype counterparts, have been widely documented (29) and have become a major force in the pandemic (24). Sixteen circulating recombinant forms (CRFs) and hundreds of unique recombinant forms (URFs), the latter being isolated only from single individuals, have been identified. Some regional epidemics are dominated by a single CRF, while others have mostly URFs. In East Africa, URFs account for 30 to 50% of infections, while CRFs have been rare (3, 8, 15, 17). Epidemics in which CRFs dominate include those in West and West Central Africa, where CRF02_AG accounts for at least 50% of infections (22), and Southeast Asia, where CRF01_AE is the predominant strain (39).

Approaches for the molecular epidemiology of HIV-1 have been progressively adapted to better detect coinfections and recombination. The complete sequencing of HIV-1 genomes has led the effort to characterize recombinant strains (6, 30, 38). Multiregion hybridization assays (MHAs) provide an accurate, high-throughput, and less labor-intensive approach to the detection of recombinants and coinfected individuals. Three different MHAs are in development (16, 22; G. Kijak, S. Tovanabutra, et al., Abstr. XV Int. AIDS Conf., abstr.

* Corresponding author. Mailing address: U.S. Military HIV Research Program, 1600 E. Gude Drive, Rockville, MD 20850. Phone: (301) 251-5065. Fax: (301) 762-7460. E-mail: fmccutchan@hivresearch.org.

† Supplemental material for this article may be found at http://jvi.asm.org/.

MoPeC3415, 2004), with each tailored to the mixture of subtypes in a specific geographic region. MHAs provide the capacity to accurately genotype hundreds of samples in a short time period, permitting comprehensive comparisons of different populations and epidemics. Recent work in Tanzania has shown an association between the risk for HIV-1 infection, HIV-1 prevalence, the proportion of strains that are URFs, and the fraction of individuals that may be coinfected with multiple subtypes (4; M. Hoelscher, M. Arroyo, et al., Abstr. AIDS Vaccine 04, abstr. 21, 2004; K.-H. Herbinger, M. Gerhardt, et al., submitted). Clearly, coinfection in populations is a potential source of rapid viral evolution by recombination and an increasing genetic complexity of strains, and some of the tools are in place to determine the impact of coinfection on HIV-1 epidemics and on infected individuals.

More recently, the parameters of HIV-1 coinfection and recombination at the level of the infected cell have been better defined. The demonstration that infected cells harbor multiple proviruses in their genome was an important milestone because it confirmed that the conditions for interstrain recombination are met at the cellular level (21). By the incorporation of fluorescent reporter genes into HIV-1 strains, it has become possible recently to directly measure rates of recombination, and the parameters that affect these rates, in an in vitro system (25). The number of crossovers per replication cycle is much higher than previously thought, estimated at 9 per replication round in T lymphocytes and up to 30 per round in macrophages. The same study showed that multiple infections of cells occur freely and that the generation of recombinants is proportional to the square of the infection rate.

The large proportion of unique recombinant forms in some mixed-subtype epidemics, which can exceed 50% of strains, is suggestive, if not prima facie, evidence that coinfection does occur at an appreciable frequency. A recent mathematical model suggests that even a low rate of coinfection would be sufficient to explain an accumulating, substantial fraction of recombinant strains in an epidemic (14). The major gaps in knowledge are the circumstances that permit coinfection to occur and the dynamics of viral evolution in coinfected individuals.

To date, there have been several well-documented HIV-1 superinfections, and because of their implications for antiviral immunity and vaccines, these reports have precipitated considerable analysis and debate (1, 10, 12, 26). The first report concerned an individual with MSM (men having sex with men) risk who was initially infected with CRF01_AE and later acquired subtype B (20). The interval between infection and superinfection was about 2 years. Two other MSM with superinfection were reported shortly thereafter, but both of these, initially infected with subtype B, acquired a second subtype B strain, one 4 months and the other 32 months after initial infection (2, 23). Two injecting drug users (IDUs) with superinfection were detected in Thailand (34), one of whom acquired subtype B within 3 months of CRF01_AE infection and the other of whom acquired CRF01_AE almost 3 years after an initial infection with subtype B. All of these superinfected individuals were at high risk for exposure to multiple HIV-1 strains or subtypes. The two cases of IDUs were the result of systematic surveillance in a cohort of 130 individuals, whereas those in MSM were identified because of clinical parameters such as an abrupt elevation in viral load during treatment or the emergence of new drug-resistant strains.

Here we report a comprehensive analysis of a superinfected individual, identified in Africa in the context of a well-designed and systematic cohort study of 600 individuals with heterosexual risk, the HIV Superinfection Study (HISIS). The approaches that permitted the successful development and retention of this cohort, as well as some of its social and behavioral characteristics, have been reported (18, 35). Other pending reports from HISIS include descriptions of HIV-1 infection in the cohort and its parameters (M. Hoelscher, O. Hoffmann, et al., submitted for publication) and of other coinfected individuals who were also studied in substantial molecular detail (11; S. Piyasirisilp, S. Tovanabutra, et al., unpublished data). Participant 123, who is the subject of this report, was ascertained in the seronegative window period, after HIV-1 infection but before seroconversion, and was identified as a potential superinfection case by MHAacd genotyping every 3 months for 30 months.

MATERIALS AND METHODS

HIV-1 serodiagnosis. HIV-1 diagnosis was done with Enzygnost Anti-HIV1/2 Plus (Dade Behring, Liederbach, Germany) and Determine HIV1/2 (Abbot, Wiesbaden, Germany) tests.

Verification of sample identity. Serial samples from participant 123 and other participants were recoded and analyzed using an AmpFLSTR Profiler Plus PCR amplification kit (Applied Biosystems, Foster City, CA) on DNAs extracted from primary peripheral blood mononuclear cells (PBMC). The alleles at nine short tandem repeat loci were identical in the 10 serial samples from participant 123.

Plasma viral load. Plasma viral loads were determined with RNAs extracted from plasma using the Amplicor HIV-1 MONITOR test, version 1.5 (Roche Molecular Systems, Branchburg, N.J.).

Lymphocyte immunophenotyping. Specimens were drawn in EDTA, kept at room temperature, and stained within 24 h of venipuncture. Trucount tubes (Becton Dickinson, San Jose, CA), which contain a bead pellet, were used in order to determine the absolute counts as well as the percentages of lymphocyte subsets within each specimen. Two Trucount tubes were prepared for each specimen by adding 10 μl of either of the following four-color antibody cocktails: (i) CD3-fluorescein isothiocyanate, CD8-phycoerythrin, CD45-peridinin chlorophyll A protein (PerCP), and CD4-allophycocyanin or (ii) CD3-fluorescein isothiocyanate, CD56+16-phycoerythrin, CD45-PerCP, and CD19-allophycocyanin. Fifty microliters of anticoagulated blood was added using the reverse pipetting method. The tubes were vortexed and incubated for 15 min at room temperature in the dark. FACSlyse (450 μl) was added to each tube to lyse the red blood cells, and the tubes were incubated as before. The stained specimens were analyzed on a Becton Dickinson FACSCalibur cytometer to determine the percentages and absolute counts of lymphocyte subsets ($CD3^+$ $CD4^+$, $CD3^+$ $CD8^+$, B, and NK cells).

Virus isolation. The target cells for virus isolation were prepared by thawing cryopreserved HIV-negative donor PBMC and performing depletion of the $CD8^+$ cells using immunomagnetic selection per the manufacturer's instructions (Dynal, Inc.). The CD4-enriched target cells were stimulated with phytohemagglutinin (PHA) for 3 days; the PHA was then washed out, and cells were maintained in cRPMI (RPMI 1640 medium supplemented with 15% heat-inactivated fetal bovine serum, 1% penicillin-streptomycin, and 20 mM L-glutamine) containing 20 IU/ml recombinant interleukin-2 (IL-2) (cRPMI/IL-2) during all subsequent culture periods. The visit 1 virus isolate from patient 123 was obtained by incubating 200 μl of patient plasma with 2×10^6 $CD4^+$ target cells for 6 h. The plasma was then washed out, and the cells were cultured for 3 weeks in cRPMI/IL-2. Virus expression in culture fluids was monitored every 3 to 4 days by a p24 antigen capture assay (Beckman-Coulter, Miami, FL); virus aliquots were harvested at or near the peak of p24 production and stored in liquid nitrogen. The cultured cells expressing the patient 123 visit 1 virus were cryopreserved at −80°C.

Nucleic acid extraction. PBMC DNA or DNA from virus culture was extracted using QIAamp blood extraction kits (QIAGEN, Valencia, CA) or a MagNaPure LC DNA isolation kit on a MagNaPure LC instrument (Roche Diagnostics Corp., Indianapolis, IN) per the manufacturer's instructions. Viral RNAs were

extracted from plasma using Roche Amplicor version 1.5 (Roche Molecular Systems, Branchburg, NJ).

MHAacd. The MHAacd used for this study was performed as described previously (3, 16), using DNA extracted from primary PBMC. Briefly, in the first-round PCR, five short amplicons distributed across the HIV-1 genome were produced. Second-round amplification was done in the presence of subtype-specific fluorescent probes using an ABI 7700 sequence detection system. Each first-round product was amplified in three second-round PCRs, each conducted in the presence of a different subtype-specific probe.

PCR. Table S1 in the supplemental material lists the PCR primers used for this study, together with their locations in reference strain HXB2 and the temperatures used for annealing or reverse transcription. The PCR conditions and cycling parameters were as follows.

(i) DNA PCR of *gag* and *gp41*/*nef*. The *gag* (HXB2 positions 892 to 2272) and *gp41*/*nef* (HXB2 positions 7745 to 9037) regions of HIV-1 viral quasispecies were retrieved by nested PCRs using two different outer and inner primers in four different pairwise combinations. First-round PCRs were conducted in 50-μl mixtures with 5 μl of 10× PCR Gold buffer (Applied Biosystems Inc., Foster City, CA), a 200 μM concentration of each deoxynucleoside triphosphate (dNTP), 1.5 mM $MgCl_2$, a 0.4 μM concentration of each primer, 0.75 U of Ampli*Taq* Gold DNA polymerase (Applied Biosystems Inc.), and 5 to 10 μl of DNA template. The cycling conditions for the first round were 1 cycle at 95°C for 10 min; 35 cycles of 95°C for 10 s, the annealing temperature for 30 s, and extension at 72°C for 2 min; and a final extension at 72°C for 10 min. The second-round PCRs contained similar final concentrations in the PCR mixtures, but with 1 μl of the pooled first-round products from two different outer primer pairs, and the number of repeat cycles was 30. The sequences of the primers and the annealing temperatures used are given in Table S1 in the supplemental material.

(ii) RT-PCR of *gag* and *gp41*/*nef*. RNAs were extracted as for the Roche Amplicor version 1.5 viral load assay (ultrasensitive method) and were the template for reverse transcription-PCR (RT-PCR) with a QIAGEN one-step RT-PCR kit (QIAGEN Inc., Valencia, CA) as instructed by the manufacturer. The primer pairs used for the first-round RT-PCR and DNA PCR in each region were the same as the primers used for the first-round DNA PCRs described above, as shown in Table S1 in the supplemental material. A reverse transcription step at 50°C for 30 min was followed by DNA PCR cycling conditions as described above, except that the initial time at 95°C was increased to 15 min to inactivate reverse transcriptase and activate Hot Start *Taq* DNA polymerase. The second-round PCR was performed as described above.

(iii) RT-PCR of *gp160*. Extracted RNAs were subjected to RT-PCR using an Invitrogen SuperScript III for RT-PCR kit (Invitrogen Corp., Carlsbad, CA) as instructed by the manufacturer. Briefly, an RNA-primer mix containing up to 5 μl RNA, 2 μl of 10 mM dNTPs, 1 μl of primer JL89 (50 mM), and diethylpyrocarbonate-treated water to make up a 10-μl reaction volume was incubated at 65°C for 5 min. Ten microliters of cDNA synthesis mix containing 2 μl of 10× RT buffer, 4 μl of 25 mM Mg_2Cl, 2 μl of 0.1 M dithiothreitol, 40 U of RNaseOUT, and 200 U of SuperScript III reverse transcriptase was added. The mixture was then incubated at 50°C for 2 h and at 85°C for 5 min to terminate the reaction. The synthesized cDNAs were chilled on ice and subjected immediately to DNA PCR. DNA PCRs were performed using previously described procedures (31). The primers for the first-round PCR were JL 86 and JL89, and the second-round primers were ED3 and JL88TA (see Table S1 in the supplemental material).

Molecular cloning. (i) *gag* and *gp41*/*nef*. The four PCR products obtained from DNA amplification of *gag* or the four products from *gp41*/*nef* amplification were combined and concentrated using Microcon YM-50 centrifugal filters (Millipore Corp., Billerica, MA), purified, and cloned into the pCR2.1-TOPO vector using a Topo TA cloning kit and TOP10 one-shot chemically competent cells as instructed by the supplier.

(ii) *gp160*. The purified *gp160* PCR product was concentrated using Microcon YM-50 filters, purified, and cloned into the pCRXL-TOPO vector using a Topo XL PCR cloning kit and MAX Efficiency Stbl2 competent cells (Invitrogen Corp., Carlsbad, CA) as instructed by the supplier.

DNA sequencing. Plasmid DNAs were extracted using a Qiawell 8 ultraplasmid kit (QIAGEN, Valencia, CA). At least 20 clones from each genome region were sequenced using BigDye Terminator v. 3.1 cycle sequencing kits and an ABI 3100 capillary sequencer (Applied Biosystems Inc., Foster City, CA). DNA sequences were assembled using Sequencher software, version 4.2 (Genecodes Inc., Ann Arbor, MI).

Phylogenetic analysis. DNA sequences were aligned with reference sequences of important HIV-1 subtypes and CRFs. Phylogenetic analysis was done with the SEQBOOT, DNADIST (Kimura 2 parameter; transition/transversion ratio, 2.0), NEIGHBOR, and CONSENSE modules of PHYLIP (9). Trees were generated with Treetool (27). A subtype J sequence was used as the outgroup root. Recombinant strains were identified and mapped by bootscanning (37) using maximum parsimony and a sliding window of 300 nucleotides (nt) overlapping by 20 nt. Subregion trees were used to confirm subtype assignments and were generated as described above, except that representative sequences of the molecular forms under analysis were used instead of the complete data set. All sequences derived from visits 0, 1, and 2 are represented with open symbols in the figures, and sequences from visit 3 or later are shown with closed symbols. All scale bars represent a 10% difference. The numbering of breakpoints was done according to the reference strain HXB2 (www.hiv.lanl.gov).

Viral strain-specific PCR. To differentiate between initial and superinfecting HIV-1 strains, strain-specific primers were designed based on the known sequences, and flanking, outer primers were designed using sequences common to the two strains. The primers and their annealing temperatures are shown in Table S1 in the supplemental material. DNA PCRs were conducted in a final volume of 50 μl containing 5 μl of 10× PCR Gold buffer, a 200 μM concentration of each dNTP, 1.5 mM Mg_2Cl, a 400 nM concentration of each primer, and 0.5 U of Ampli*Taq* Gold DNA polymerase. One microliter of the first-round products was used as the template for second-round PCR. The cycling conditions were as follows: 1 cycle at 95°C for 10 min; 35 cycles of 95°C for 10 s, the annealing temperature for 30 s, and extension at 72°C for 2 min; and a final extension at 72°C for 10 min.

GenBank sequence accession numbers. The sequences obtained in this study have been contributed to GenBank. The complete genome has the accession number AY945709. The accession numbers for *gp160* from visit 1 plasma are AY887501 to AY887515, and those for *gp160* from visit 3 plasma are AY887516 to AY887535. The accession numbers for *gp41*/*nef* sequences are as follows: AY887287 to AY887379, form I; AY887380 to AY887427, form II; AY887428 to AY887433, form III; AY887434 to AY887435, form IV; AY887436 to AY887499, form V; and AY887500, form VI. The *gag* sequences are found under the following accession numbers: AY887175 to AY887253, form I; AY887254 to AY887255, form II; AY887256 to AY887261, form III; AY887262 to AY887263, form IV; AY887264 to AY887281, form V; AY887282, form VI; and AY887283 to AY887286, form VII. See Table S2 in the supplemental material for additional details.

RESULTS

HISIS and participant 123. Dual infections with two or more HIV-1 subtypes are being systematically evaluated in the Mbeya region of Southwestern Tanzania. Based on a behavioral and demographic study throughout the region (18), 600 female bar workers have been enrolled in HISIS and monitored every 3 months for more than 3 years. The participants are at high risk for HIV-1 infection and are exposed to subtypes A, C, D, and their recombinants. At baseline, almost 70% were HIV-1 seropositive, and the HIV-1 incidence in the first year of follow-up was 14%. Through a combination of risk reduction counseling, condom promotion, and treatment of other sexually transmitted infections, the HIV-1 incidence dropped significantly in years 2 and 3 of the study (M. Hoelscher, O. Hoffmann, et al., unpublished data).

To detect dual infections, a genetic screening assay, the MHAacd, was applied to serial samples from almost 200 HISIS participants. This assay evaluates the genetic subtype in multiple regions along the genome with subtype-specific fluorescent probes. The overall results of genetic screening for HISIS and confirmation and characterization of several other dual-infection cases will be reported elsewhere (11; S. Piyasirisilp, D. Mloka, et al., unpublished data). Participant 123, who is the subject of this report, was selected for in-depth genetic analysis because she was enrolled in the study during the seronegative window period shortly after infection and showed two indications of dual infection, namely, a shift in subtype over time and

TABLE 1. Sampling, clinical parameters, and HIV-1 genotyping

Visit	Time of visit (mo)	HIV-1 serostatus	Plasma viral load[a] (copies/ml)	Clinical symptoms	No. of CD4 cells/μl of plasma[b]	No. of CD8 cells/μl of plasma[b]	MHA genotype[c]				
							gag	*pol*	*vpu*	*env*	gp
0		Negative	3.6×10^3	Healthy	ND	ND	—	—	—	—	—
1	3	Positive	2.1×10^6	Healthy	ND	ND	A	A	C	—	D
2	6	Positive	4.9×10^5	Malaise, decreased appetite, lymphadenitis	ND	ND	—	—	C	—	—
3	9	Positive	4.0×10^5	Recurring episodes of short fever, cough and diarrhea, moderate weight loss	ND	ND	A	C	C	A	ACD
4	12	Positive	6.9×10^4		ND	ND	A	C	C	A	ACD
5	15	Positive	6.6×10^4		ND	ND	A	C	C	A	ACD
6	18	Positive	2.9×10^5		ND	ND	A	C	C	A	ACD
7	21	Positive	7.2×10^4		ND	ND	A	C	C	A	AD
8	24	Positive	6.5×10^4		482	587	A	C	C	A	ACD
9	27	Positive	7.5×10^4		ND	ND	A	C	C	A	ACD
10	30	Positive	4.8×10^4		377	448	A	C	C	A	ACD

[a] Samples from visits 1, 2, 3, and 6 were analyzed with the Roche v.1.5 standard assay; other visits were analyzed with the Roche v.1.5 ultrasensitive assay.
[b] ND, not done.
[c] Determined by MHAacd as described in reference 13 and modified in reference 3. gp, gp41; —, none of the three subtype-specific probes hybridized.

multiple probes hybridizing in a single genome region. Clinical parameters and MHAacd genotypes are shown in Table 1.

Samples were drawn from the baseline and 10 follow-up visits, spanning 30 months. At baseline, participant 123 was HIV-1 seronegative with a plasma viral load of 3.6×10^3 copies/ml, and the MHAacd was negative for DNA extracted from primary PBMC. At 3 months, she was HIV-1 seropositive, had a plasma viral load of $>2 \times 10^6$ copies/ml, and harbored an ACD recombinant genotype in PBMC. The viral load remained high until 12 months, when a set point at 6.7×10^4 copies/ml was achieved and generally maintained. Visit 2, which occurred 6 months after enrollment, marked the beginning of clinical symptoms consistent with a recent HIV-1 infection, and throughout the subsequent months of study, participant 123 experienced repeated health problems. Her CD4 cell count was 482 cells/μl after 24 months of follow-up and had declined to 377 cells/μl by 30 months. MHA genotyping was incomplete at 6 months but was consistently achieved thereafter. Importantly, the subtype shifted from A to C in a region at the end of *gag* which overlaps with the *pol* reading frame (Table 1), and at the same visit, multiple probes began to hybridize to the *gp41* region of the envelope, where only the subtype D probe hybridized initially. The serial samples from this participant were verified independently using Profiler (see Materials and Methods), confirming that different MHA genotypes evolved in a single individual over time. These results suggested that participant 123 was infected with an ACD recombinant HIV-1 strain shortly before the baseline visit and became superinfected with one or more additional HIV-1 strains between 3 and 9 months of follow-up.

Sampling the viral quasispecies. Evaluations of dual HIV-1 infections require adequate sampling of the viral quasispecies, because the proportions of strains may be unequal and fluctuating. For primary PBMC or plasma, the strategy employed throughout this study was to PCR amplify a genome region of interest with two sets of outer primers and two sets of inner primers used in four pairwise combinations. PCR products from the four separate amplifications were combined and molecularly cloned, and individual clones, usually 20 or more per sample, were sequenced. The genome regions selected for study included the complete *gp160* gene (2.5 kb), a 1.4-kb region encompassing most of *gp41* and the beginning of *nef*, and a 1.3-kb amplicon including most of *gag*. Also, a complete genome sequence was obtained using DNA from a virus culture.

Initial strain. Genetic analysis was initiated with the plasma sample from the first seropositive visit, when the viral load was at its highest observed level. Virus isolation was achieved by coculture with PHA-stimulated primary donor PBMC, and DNA from the culture was the template for complete HIV-1 genome amplification by limiting-dilution nested PCR and for sequencing. The strain was a complex ACD recombinant with 12 breakpoints across the genome (Fig. 1). Each of the 13 genome regions demarcated by the breakpoints was analyzed separately (Fig. 1, trees I to XIII) to confirm the subtype. The first segment, encompassing *gag* and the first half of *pol*, was subtype A. The subtype switched to C, then to D, and back to C near the end of *pol*. In the mid-genome accessory gene region, there were several closely spaced shifts in a complex mosaic pattern of subtypes C, D, and A. The *env* gene was mosaic, with four crossovers, and included segments of subtypes C, A, and D. The first half of *nef* was subtype D.

Envelope genes of initial and superinfecting strains. HIV-1 *env* genotypes in the plasma compartment were investigated at the first seropositive visit (visit 1) and at visit 3, when the genotype had shifted in the MHAacd assay (Table 1). Figure 2A shows the results of a phylogenetic analysis of 15 and 20 plasma-derived clones from visits 1 and 3, respectively. At visit 1, the quasispecies was highly homogeneous (open circles; mean pairwise nucleotide sequence distance, 0.5%), and all sequences clustered with a bootstrap value of 100%. The *env* gene from the visit 1 virus culture (Fig. 2A, arrow) was nearly

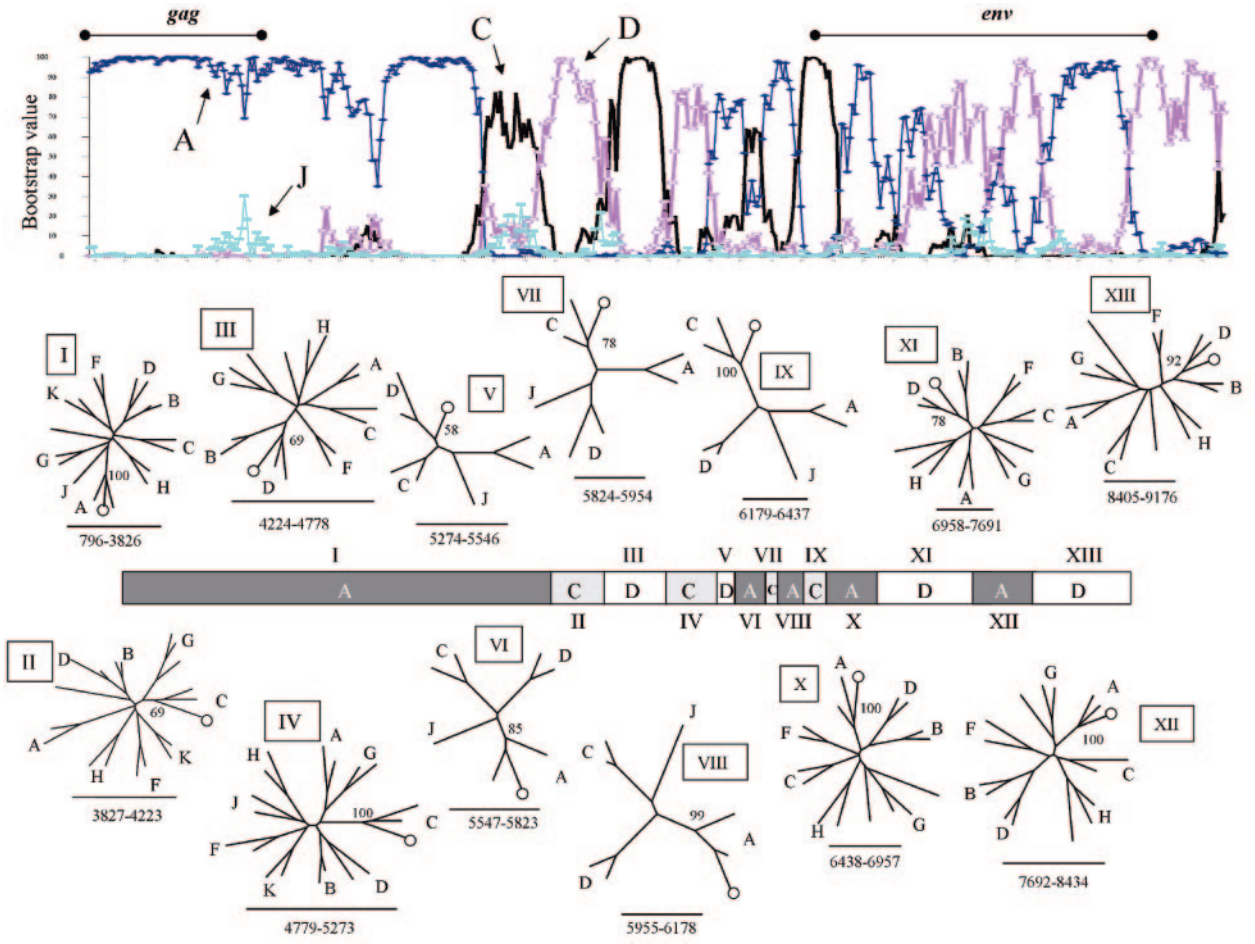

FIG. 1. Recombinant structure of the initial strain. A virtually complete HIV-1 genome sequence from participant 123 was analyzed by bootscanning with subtype A, C, D, and J reference sequences. The top panel shows the maximum parsimony bootstrap values for subtype associations across the genome. Subregions of different subtypes (I through XIII) were excised and analyzed with reference sequences of all subtypes using neighbor joining with the bootstrap. The position of the 123 strain (open circle) and bootstrap support for subtype assignments are indicated. The boundaries of each segment are delineated according to positions in reference strain HXB2. The diagram in the center summarizes the recombinant structure.

identical to sequences recovered from visit 1 plasma. At visit 3, a different, but also highly homogeneous, strain (mean pairwise nucleotide sequence distance, 1.0%) was found, again clustering together with a 100% bootstrap value (filled circles). In this case, two subfamilies of sequences could be discerned (variant 1 and variant 2, including 13 and 7 sequences, respectively), each of which was supported by significant bootstrap values. The visit 1 and visit 3 strains differed by 15.5% at the nucleotide level. Both strains formed deep branches in subtype A. The translated protein sequences of these strains differed by 25.6%. The regions of greatest divergence were V1 through V5 and the cytoplasmic domain of gp41. Variants 1 and 2 from visit 3 were quite similar, differing at 25 positions scattered throughout the envelope (see Fig. S2 in the supplemental material).

The visit 1 and visit 3 *env* genes were analyzed by bootscanning, and both were found to be recombinant. Their structures are compared in Fig. 2B. The visit 1 envelope was an ACD recombinant which was identical in structure to that found in the complete genome sequence. The envelope at visit 3 was an AC recombinant with four crossover points. Subregion trees confirmed the structure of the visit 3 envelope and verified that variants 1 and 2 had the same AC recombinant structure (see Fig. S1 in the supplemental material). Interestingly, the visit 1 and 3 envelope genes had two breakpoints in common, within the precision afforded by bootscanning, at position 6957 and position 8434 (HXB2 numbering), respectively. Regions that were the same subtype in the two envelopes were then compared (Fig. 2B, center panel). While both envelope genes began with a subtype C segment, these were from different subtype C lineages, since the sequences from the two time points clustered separately and the branch lengths separating them were typical for other pairs of unrelated subtype C strains. Similarly, the two subtype A regions that could be compared were from different subtype A lineages. It was concluded that the envelopes of the strains recovered at visits 1 and 3 were unrelated recombinants, i.e., one ACD recombinant and one AC recombinant.

Temporal evolution of *gp41*/*nef* in the viral quasispecies. The genetic analysis of the superinfection was extended to

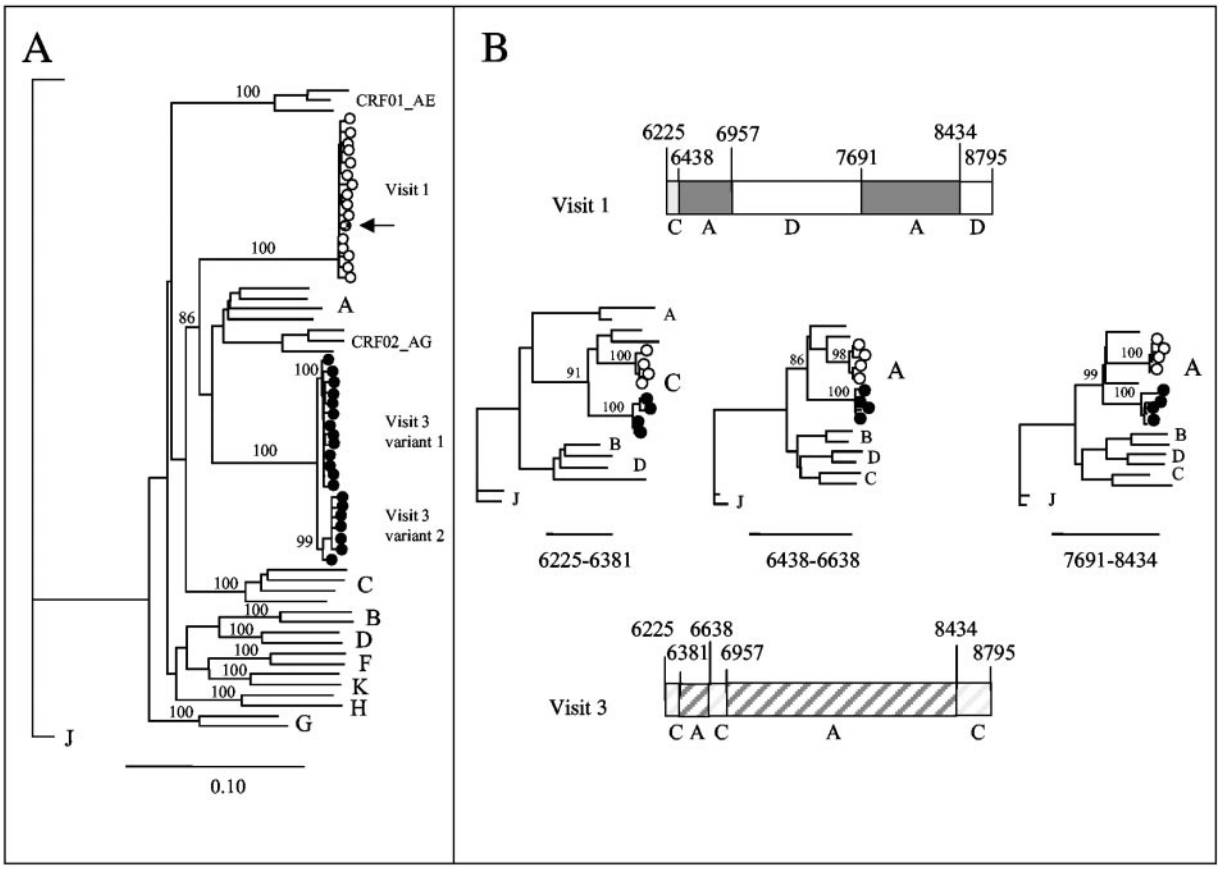

FIG. 2. Envelope sequences before and after superinfection. (A) Plasmas from visits 1 and 3 were the source of complete envelope sequences, represented by open and filled circles, respectively. The open circle indicated by the arrow is the corresponding sequence from the complete genome shown in Fig. 1. For visit 3, two related but distinct variants were found, i.e., variants 1 and 2. The tree was constructed by neighbor joining with the bootstrap, and the scale bar represents a 10% difference. Bootstrap values at important nodes are indicated. A subtype J sequence was designated as the outgroup root. (B) Recombinant structures of the envelopes present at visit 1 and 3 are shown, with breakpoints numbered according to positions in strain HXB2. The center panel compares regions of the same subtype in the two recombinants, using selected clones from visits 1 and 3 (open and filled circles, respectively). Visit 1 and visit 3 strains clustered separately within their subtype, indicating different lineages, which are represented by shading or crosshatching, respectively.

include additional visits, using plasma as the source of viral RNA and a 1.4-kb amplicon encompassing most of *gp41* and the first half of *nef*. Figure 3A shows the relationships of 69 *gp41*/*nef* clones from visit 0, before seroconversion, and from visits 1 through 3. The molecular forms that were recovered are indicated with Roman numerals, and their recombinant structures are shown in Fig. 3B.

All of the clones from visits 0, 1, and 2 clustered tightly and represented form I, an AD recombinant. At visit 3, four other molecular forms were recovered, and form I was not seen. Forms III, IV, and VI were ACD recombinants, each with a different but related structure (form II, recovered only from PBMC, will be described below). Form V was an AD recombinant with essentially the same recombinant structure as form I but was a secondary recombinant with the subtype A portion from the superinfecting strain. Indeed, all of the molecular forms except for form I received their subtype A portions from the superinfecting strain. Subregion trees establishing this observation are shown in Fig. S3 in the supplemental material. The subtype D portions of all of the molecular forms derived from the initial strain, whereas the subtype C portions all derived from the superinfecting strain. Form III represents the strain recovered by *gp160* cloning of the visit 3 plasma (compare Fig. 2B, visit 3 strain, and Fig. 3B, form III), but in the *gp160* analysis by a single nested PCR, only this form was seen, whereas in the analysis of *gp41*/*nef*, where multiple primer combinations were applied, additional forms were found.

In summary, the plasma contained a highly homogeneous AD recombinant strain that was present before seroconversion and persisted for the first 6 months of infection without any appreciable diversification. At 9 months, a superinfecting strain, together with recombinants of the initial and superinfecting strain, was present, but the initial strain was not recovered among the clones analyzed.

Figure 3C shows a similar analysis using the same *gp41*/*nef* amplicon but exploring the viral quasispecies using DNAs extracted from PBMC. In this case, visits 1, 2, 3, 4, 7, and 10 were included to monitor viral evolution for 30 months after infection. Selected clones from the plasma compartment were included in the analysis, serving as markers to identify the different molecular forms. In all, 126 new clones were analyzed.

All of the molecular forms found in plasma from visits 0 to

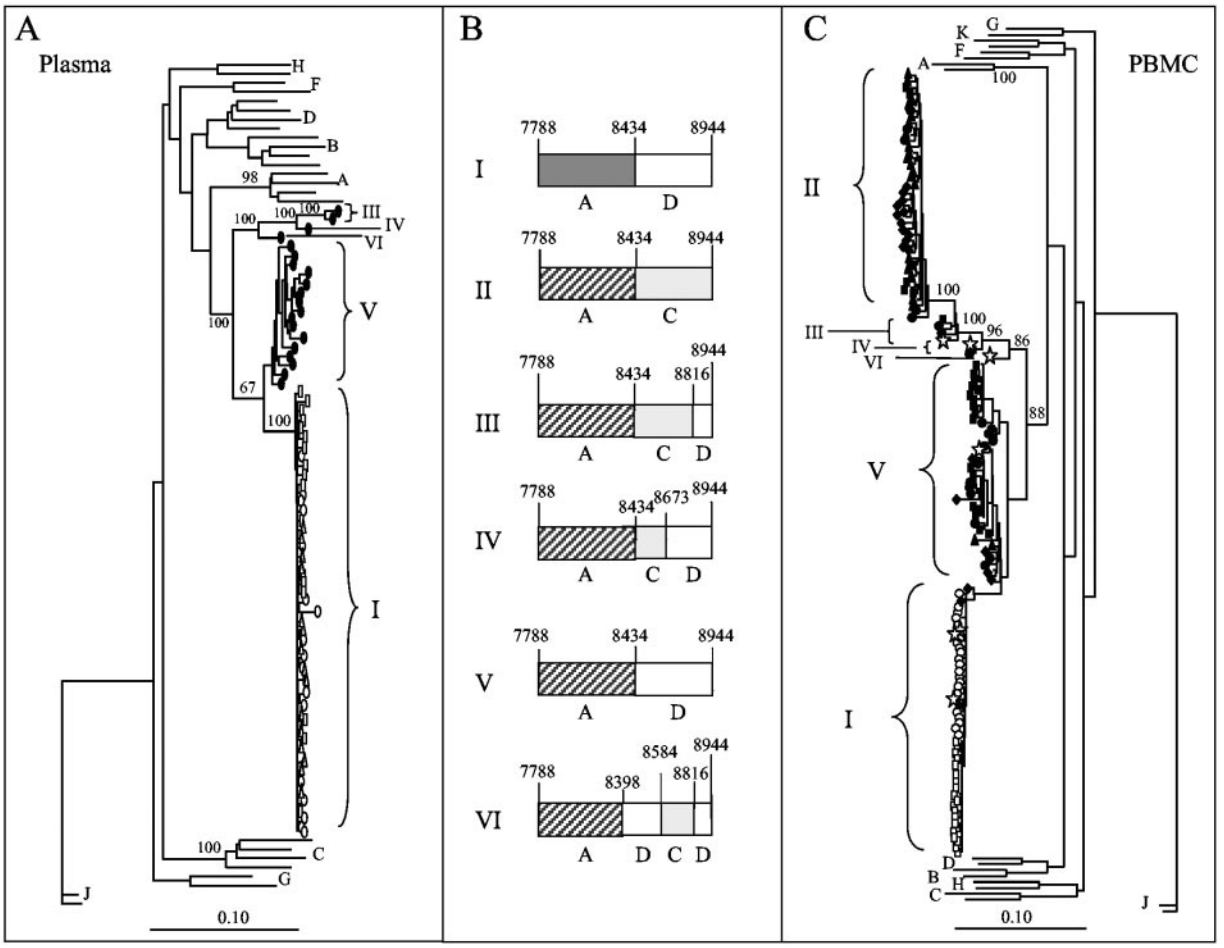

FIG. 3. Temporal evolution of *gp41*/*nef* recombinant forms in plasma and PBMC. (A) The source of *gp41*/*nef* recombinant sequences was RNA extracted from plasma. The phylogenetic tree was constructed by neighbor joining, including *gp41*/*nef* sequences from visits 0, 1, 2, and 3 (open triangles, open circles, open squares, and closed circles, respectively) and reference sequences of relevant subtypes. Bar, 10% difference. Bootstrap values at important nodes are indicated. The different molecular forms are indicated by Roman numerals. (B) Structure of recombinant forms with breakpoints indicated (HXB2 numbering). For the subtype A segments, shading indicates regions from the initial strain; crosshatched regions are from the superinfecting strain. (C) The source of *gp41*/*nef* recombinant sequences was DNA extracted from PBMC. The phylogenetic tree was constructed by neighbor joining, including *gp41*/*nef* sequences from visits 1, 2, 3, 4, 7, and 10 (open circles, open squares, closed circles, closed triangles, closed squares, and closed diamonds, respectively) and reference sequences of relevant subtypes. Bar, 10% difference. Bootstrap values at important nodes are indicated. Stars represent sequences from plasma (panel A) representing forms I, III, IV, V, and VI, respectively. Form II was found only in PBMC.

3, except form VI, were also found in PBMC, together with an additional form, form II. Form I, the initial strain, was the only form found for visits 1 and 2. In parallel with the case for the plasma compartment, form I was not found at visit 3 but was occasionally detected later, in one clone at visit 4 and two clones at visit 10. It is highly likely that form II represents the superinfecting strain, since all of the other forms can be derived by recombination between forms I and II. Figure S3 in the supplemental material contains the subregion trees confirming the structure of form II. Form II was found in PBMC from visits 3, 4, 7, and 10. Forms III, IV, and V found in plasma were also present in PBMC, and as in plasma, form V was the most abundant of these at visit 3 but was also substantially represented at later time points. Forms III and IV were of low abundance in both PBMC and plasma. These data indicate that within 3 months of superinfection, multiple recombinant forms derived from the initial and superinfecting strains were generated. At the same time, there was a significant rebalancing of the viral quasispecies in both PBMC and plasma. Neither the plasma nor the PBMC compartment showed evidence of the presence of the superinfecting strain (form II) prior to visit 3. The superinfecting strain was apparently present quite transiently in the plasma and was quickly replaced by a dominant recombinant strain, form V, and other recombinants.

Are the proportions of molecular forms recovered from the various visits and compartments significantly influenced by sampling? This question was addressed using visit 3 PBMC, in which the quasispecies was heterogeneous and the molecular forms were present in highly unequal proportions. The visit 3 DNA sample was amplified and cloned a second time, using the same method as before, and the proportions of molecular forms in the two samples were compared. The three most abundant forms, II, III, and V, were recovered in similar, if not identical, proportions in samples 1 and 2. The less abundant

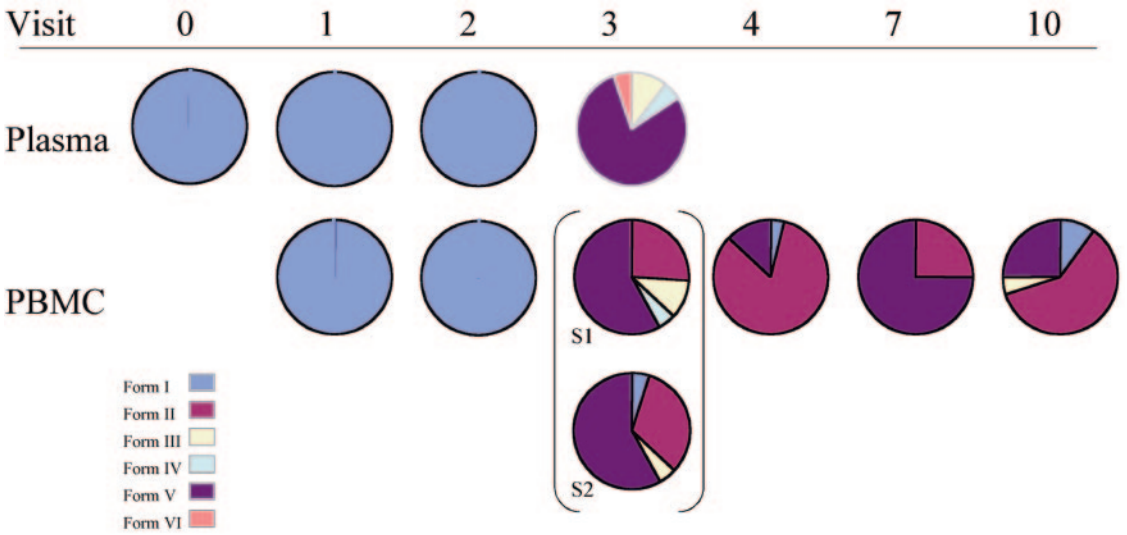

FIG. 4. Consistency of sampling and temporal fluctuation of molecular forms in plasma and PBMC. The compositions of the viral quasispecies in plasma and PBMC from visit 0 through visit 10 are shown, comparing sequences obtained from plasma RNA with those obtained from PBMC DNA. Each pie chart represents approximately 20 sequences. The legend indicates the colors used to represent the various molecular forms. Form I is the initial form, and form II is the superinfecting strain; all other forms are recombinants of these. At visit 3, the PBMC compartment was independently sampled (S1 and S2) to compare the proportions of forms recovered.

forms I and IV were not as consistently sampled (see Fig. S4 in the supplemental material). Notably, the second sample permitted recovery of a form I clone, representing the initial strain, from visit 3. This was the only form I clone found among 20 *gp160* and 20 *gp41/nef* clones from visit 3 plasma and among 38 *gp41/nef* clones from PBMC.

The temporal evolution of the quasispecies in plasma and PBMC is summarized in Fig. 4. For both compartments, only form I was recovered from the time of infection until visit 3. A heterogeneous new quasispecies appeared at visit 3, in which the predominant strain was form V, a recombinant between the initial and superinfecting strains. Form II, the superinfecting strain, was abundant in PBMC but not recovered from plasma at visit 3, whereas plasma included form VI, which was not recovered from PBMC. Form IV was rare in both compartments at visit 3. From PBMC, a diverse quasispecies was recovered at visits 4, 7, and 10, including forms I, II, III, and V in fluctuating proportions. Rapid turnover of the quasispecies in PBMC was occurring after superinfection. The obvious imbalance between PBMC and plasma samples from visit 3 is also noteworthy.

Temporal evolution of *gag* in the viral quasispecies. The analysis of viral evolution in participant 123 was extended by independent sampling of another gene region, a 1.4-kb amplicon encompassing most of the *gag* gene, to separately establish parameters of viral evolution and compare them with those established using the *gp41/nef* amplicon. Figure 5A presents an analysis with 112 *gag* clones recovered using DNAs extracted from PBMC on visits 1, 2, 3, 4, and 7. Seven molecular forms were recovered (Fig. 5B). The most abundant, form I, was subtype A. It accounted for all clones from visits 1 and 2 and for a portion of clones from all subsequent samples. The next most abundant form was form V, an AC recombinant whose subtype A parent is different from form I (see Fig. S5 in the supplemental material). All of the other forms were recombinants between forms I and V; therefore, form V is the likely superinfecting strain for *gag*. Forms II, III, IV, VI, and VII represent various recombinants between forms I and V, and these remained relatively rare in the quasispecies.

A comparison of the translated Gag proteins of the initial and superinfecting strains showed that the most diversity was found in p17 and p6, where the two strains were from different subtypes. Of interest, the most conserved portion, p24, was subtype A in both strains and differed by only 15 of 130 amino acids (see Fig. S6 in the supplemental material).

Superinfection or cotransmission? Is it possible that the superinfecting strain was transiently present and/or present at an extremely low abundance from the beginning and that this case represents cotransmission rather than superinfection? This question was addressed by the development and application of a strain-specific nested PCR assay. Figure S7 in the supplemental material shows the design of the assay and its validation with clones from the two strains. Figure 6 shows the amplification of serial samples from PBMC and plasma. For both compartments, the initial strain was easily detected from the earliest time points, whereas the superinfecting strain was not amplified until visit 3.

Contrasting dynamics of *gag* and *env* in the viral quasispecies. A comparison of *gag* and *gp41/nef* in the viral quasispecies sampled from PBMC showed that *gp41/nef* of the initial strain was virtually replaced by that of the superinfecting strain and its recombinants, whereas the *gag* gene of the initial strain persisted at significant levels (Fig. 7A). The portion of *gp41* that was apparently counterselected was the subtype A portion of the initial strain, encompassing the *gp41* ectodomain, which was virtually completely replaced by the corresponding portion, also subtype A, of the superinfecting strain. In contrast, the initial strain persisted for >21 months in *gag*, even constituting the majority strain at some time points. Recombinants

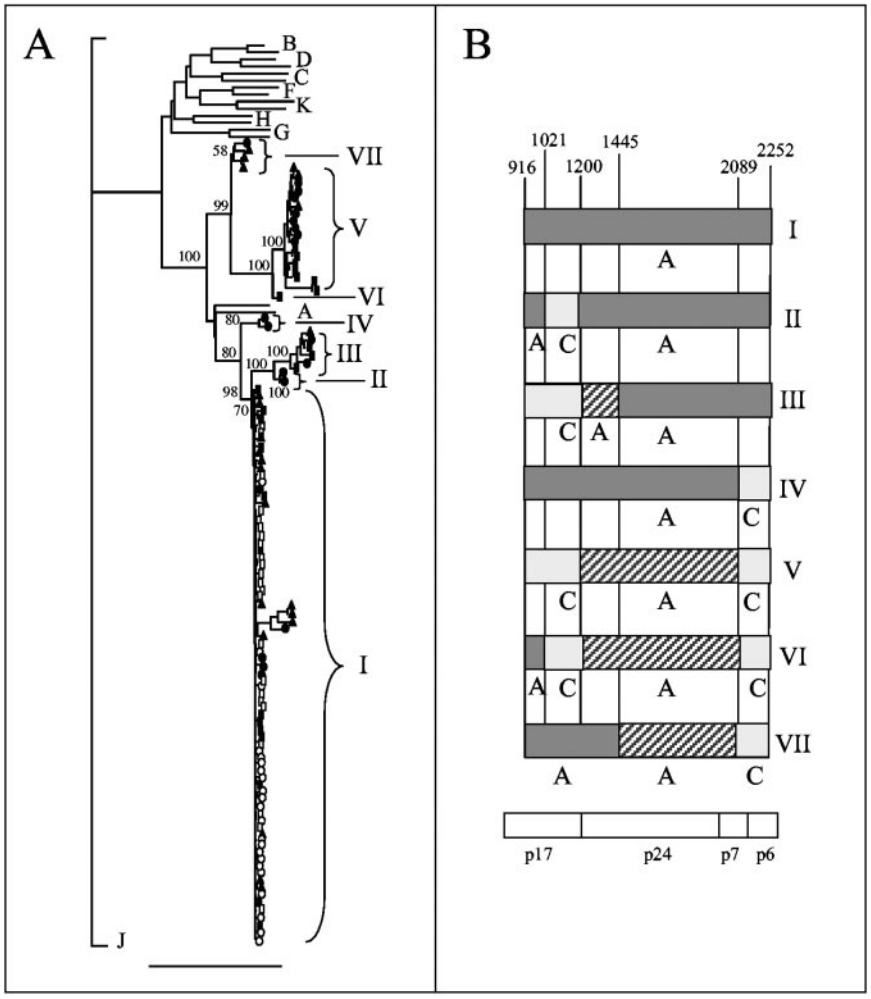

FIG. 5. Evolution of the viral quasispecies: the *gag* gene. (A) Phylogenetic tree for sequences from DNAs extracted from PBMC. The phylogenetic tree was constructed by neighbor joining, including *gag* sequences from visits 1, 2, 3, 4, and 7 (open circles, open squares, closed circles, closed triangles, and closed squares, respectively) and reference sequences of relevant subtypes. Bar, 10% difference. Bootstrap values at important nodes are indicated, and molecular forms are identified by Roman numerals. (B) Structure of recombinant forms. The subtype A portions are from two lineages, indicated by shading (initial strain) or crosshatching (superinfecting strain). The numbering of breakpoints is according to positions in HXB2. The diagram at the bottom indicates the portion of *gag* that was sequenced, from codon 43 of p17 up to 15 codons before the end of p6.

of the two strains were never in the majority for *gag*, but did dominate the quasispecies in *gp41/nef*.

Figure 7B shows how dynamic the PBMC compartment can become in the setting of superinfection and highlights the sampling issues that arise. Between visits 3 and 4, for example, the viral quasispecies in *gag* shifted from one in which the initial, superinfecting, and recombinant strains were all well represented to one in which the initial strain again dominated, while at the same time the *gp41/nef* quasispecies became dominated by the superinfecting strain. Similar shifts in proportions continued at subsequent visits. The extent of turnover of the PBMC compartment, thought to represent a relatively stable reservoir of viral strains compared to plasma, is remarkable.

Figure 7C places viral evolution in the context of the clinical picture developed for participant 123. The period of high viral load resolved to a set point between 9 and 12 months of infection. The superinfection apparently occurred approximately 3 months earlier, between 6 and 9 months of follow-up. The superinfection resulted in an explosion of viral diversity, including not only the superinfecting strain but also many recombinants derived from it, and the establishment of multiple molecular forms in PBMC and plasma occurred in less than 3 months.

DISCUSSION

This study contributes to a growing body of data suggesting that infection with HIV-1 does not necessarily protect against reinfection with another HIV-1 strain. It will be important to determine whether superinfection is the result of an immune system that is weakened or damaged by HIV-1 infection itself if HIV-1 infection in humans parallels recent work with the simian immunodeficiency virus (SIV) model system (28). An early and sometimes severe depletion of memory $CD4^+$ T cells

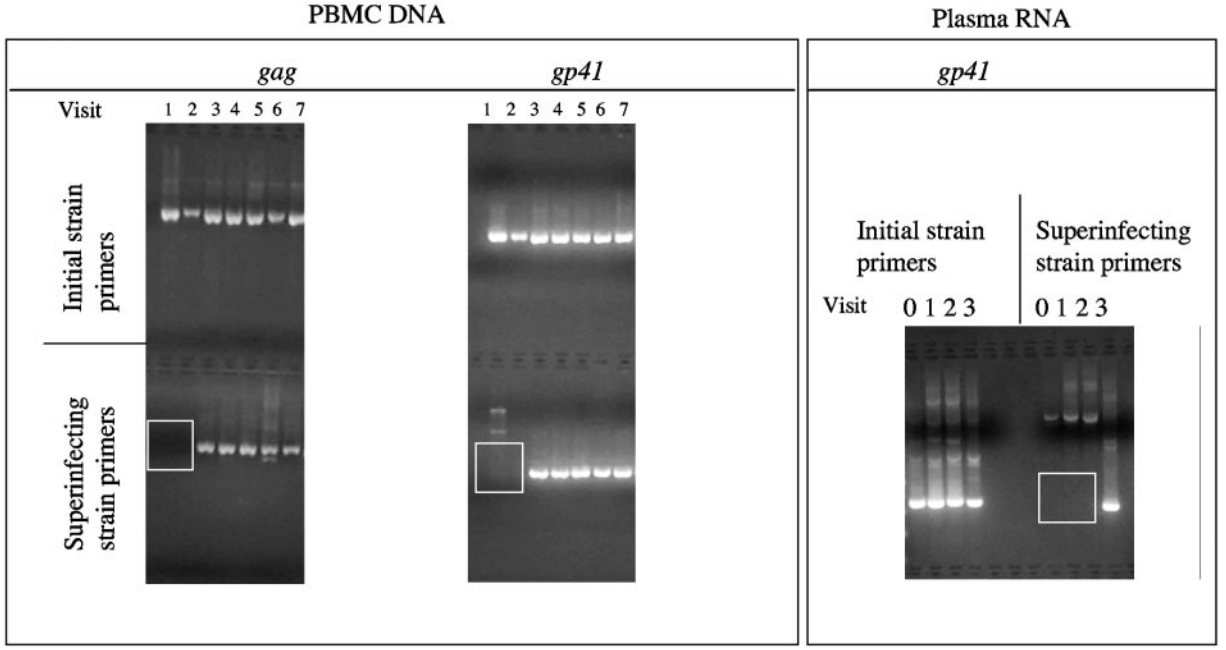

FIG. 6. Detection of initial and superinfecting strains in serial PBMC and plasma samples from participant 123 using strain-specific PCRs. (Left) DNAs from PBMC from the indicated visits were amplified in the first round with universal primers and in the second round with strain-specific primers, either for *gag* or for *gp41*. PCR products were separated in agarose gels and stained with ethidium bromide. (Right) Similarly, nested PCR was applied to RNAs from plasma samples by incorporation of an initial reverse transcription step. Boxes highlight the absence of the superinfecting strain before visit 3.

in the first weeks of infection may abrogate the defense against many pathogens, even those to which the host had established memory responses; HIV-1 superinfection may be part of this generalized immune impairment.

Alternatively, superinfection may reflect a failure of cross-protective immunity resulting from the genetic diversity of HIV-1. Superinfection might be expected to occur more readily when genetically diverse strains, such as different subtypes, challenge the already-infected host. Previous reports have documented superinfections both with strains of the same subtype and with strains of different subtypes; this report presents an intermediate case, with recombinant strains partly of the same subtype. A recent report by Yang et al. (41), like an earlier study (34), describes superinfection in an individual where T-cell responses to the initial strain were limited in the ability to recognize the superinfecting strain. However, superinfection can occur even in individuals with a broad T-cell response (2).

There is indirect evidence that participant 123 did subject the superinfecting strain to immune pressure. A key observation is the virtual replacement of the initial strain with a new recombinant in *gp41*/*nef*. The rapid turnover of the viral quasispecies in PBMC after superinfection could also reflect continuing immune pressure, or this could be the result of random expansion of latent viral variants. The fact that the superinfecting strain, which must have been vastly in the minority at the moment of superinfection, came to have a relatively high abundance in the viral quasispecies in plasma, along with recombinants derived from it, is also presumptive evidence of strong selection. Finally, participant 123 did gain control of an initially high viral load and was able to establish and maintain a set point; it is doubtful that this could have occurred without some immune control of the superinfection.

The potential public health importance of superinfection, with its capacity to rapidly generate new and potentially transmissible recombinant forms (10) and a higher viral load set point in dually infected individuals than in singly infected individuals (13), has already been noted. It appears that superinfection can generate not just one but many new recombinant forms, some of which persist at appreciable levels in the host for years. The link between dual infection and recombinant forms is now strongly forged by this and other studies, and given the established relationship between viral load and transmission (5, 32, 33), it may be that recombinants are generated in individuals who also develop higher viral loads and readily transmit them. Eventually, superinfection would be expected to increase the complexity of viral genotypes circulating in the population. Specific and concerted interventions in high-risk populations, who may be particularly susceptible to superinfection, may have a population-level as well as individual benefit.

Does HIV-1 superinfection have direct, negative implications for vaccine development? The most important data to answer this question may come from clinical trials of candidate HIV-1 vaccines in seronegative volunteers because this is the best opportunity to measure the protective effect of immune responses generated with a defined immunogen in the context of a healthy immune system. It will also be important to determine what proportion of individuals harboring two or more HIV-1 strains acquired them simultaneously at the time of first infection because these cases do not pertain to the issue of reinfection in the face of an ongoing anti-HIV-1 immune re-

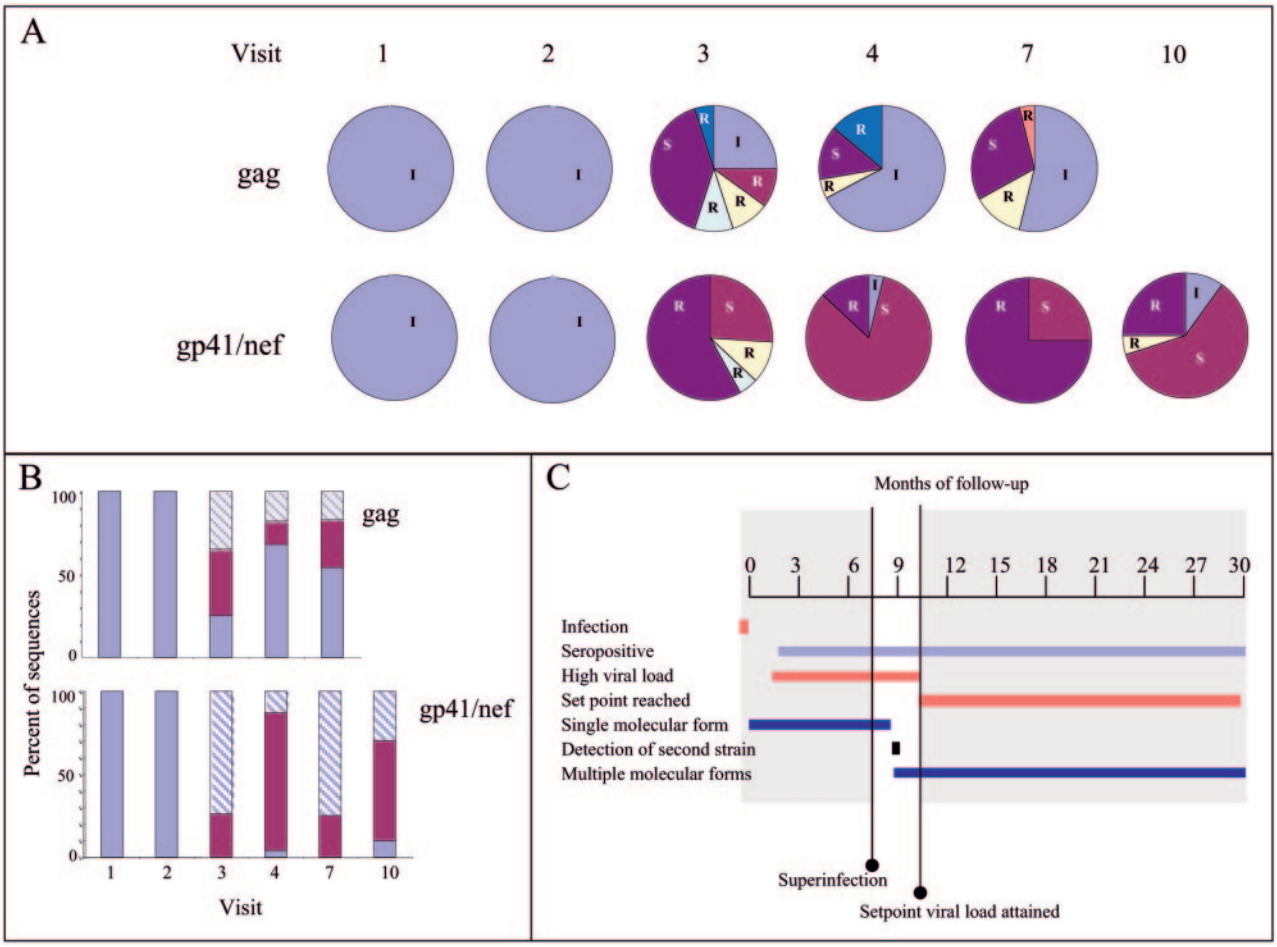

FIG. 7. Contrasting dynamics in *gag* and *env* of viral quasispecies. (A) Fluctuating proportions of molecular forms of *gag* and *gp41/nef* sampled from PBMC after superinfection. Each pie chart represents approximately 20 sequences. I, initial strain; S, deduced superinfecting strain; R, recombinant between initial and superinfecting strains. (B) Percentages of sequences that represented initial, superinfecting, and new recombinant strains (blue, magenta, and light blue, respectively) at each visit in *gag* and *gp41/nef* analyses. (C) Relative timing of initial infection, seroconversion, attainment of viral load set point, superinfection, and detection of new recombinant forms from the seronegative window period through 30 months of follow-up of participant 123.

sponse. This report and others do establish that superinfection is possible, but additional research will be needed to interpret superinfection in the context of anti-HIV-1 immunity and vaccine development.

ACKNOWLEDGMENTS

This work was supported by a cooperative agreement between the Henry M. Jackson Foundation for the Advancement of Military Medicine and the U.S. Department of Defense, by the National Institute for Allergy and Infectious Diseases, National Institutes of Health, and by the European commission, DG XII, INCO-DC.

We thank the entire HISIS team in Mbeya, Tanzania, for their careful work and all of the study volunteers for their participation.

The Walter Reed Army Institute of Research approved the manuscript for publication. The views and opinions expressed herein do not necessarily reflect those of the U.S. Army or the Department of Defense.

REFERENCES

1. **Allen, T. M., and M. Altfeld.** 2003. HIV-1 superinfection. J. Allergy Clin. Immunol. **112:**829–835.
2. **Altfeld, M., T. M. Allen, X. G. Yu, M. N. Johnston, D. Agrawal, B. T. Korber, D. C. Montefiori, D. H. O'Connor, B. T. Davis, P. K. Lee, E. L. Maier, J. Harlow, P. J. Goulder, C. Brander, E. S. Rosenberg, and B. D. Walker.** 2002. HIV-1 superinfection despite broad CD8+ T-cell responses containing replication of the primary virus. Nature **420:**434–439.
3. **Arroyo, M. A., M. Hoelscher, E. Sanders-Buell, K. H. Herbinger, E. Samky, L. Maboko, O. Hoffmann, M. R. Robb, D. L. Birx, and F. E. McCutchan.** 2004. HIV type 1 subtypes among blood donors in the Mbeya region of southwest Tanzania. AIDS Res. Hum. Retrovir. **20:**895–901.
4. **Arroyo, M. A., M. Hoelscher, W. Sateren, G. Schoen, E. Samky, L. Maboko, O. Hoffmann, E. Sanders-Buell, G. H. Kijak, M. Robb, D. Birx, and F. McCutchan.** HIV-1 diversity and prevalence differ between urban and rural areas in the Mbeya region of Tanzania. AIDS, in press.
5. **Cao, Y., P. Krogstad, B. T. Korber, R. A. Koup, M. Muldoon, C. Macken, J. L. Song, Z. Jin, J. Q. Zhao, S. Clapp, I. S. Chen, D. D. Ho, and A. J. Ammann.** 1997. Maternal HIV-1 viral load and vertical transmission of infection: the Ariel Project for the prevention of HIV transmission from mother to infant. Nat. Med. **3:**549–552.
6. **Carr, J. K., M. O. Salminen, J. Albert, E. Sanders-Buell, D. Gotte, D. L. Birx, and F. E. McCutchan.** 1998. Full genome sequences of human immunodeficiency virus type 1 subtypes G and A/G intersubtype recombinants. Virology **247:**22–31.
7. **Coffin, J. M.** 1979. Structure, replication, and recombination of retrovirus genomes: some unifying hypotheses. J. Gen. Virol. **42:**1–26.
8. **Dowling, W. E., B. Kim, C. J. Mason, K. M. Wasunna, U. Alam, L. Elson, D. L. Birx, M. L. Robb, F. E. McCutchan, and J. K. Carr.** 2002. Forty-one near full-length HIV-1 sequences from Kenya reveal an epidemic of subtype A and A-containing recombinants. AIDS **16:**1809–1820.

9. **Felsenstein, J.** 1989. PHYLIP—phylogenetic inference package (version 3.2). Cladistics **5:**164–166.
10. **Fultz, P. N.** 2004. HIV-1 superinfections: omens for vaccine efficacy? AIDS **18:**115–119.
11. **Gerhardt, M., D. Mloka, S. Tovanabutra, E. Sanders-Buell, O. Hoffmann, L. Maboko, D. Mmbando, D. Birx, F. McCutchan, and M. Hoelscher.** 2005. In-depth, longitudinal analysis of viral quasispecies from an individual triply infected with late-stage human immunodeficiency virus type 1, using a multiple PCR primer approach. J. Virol. **79:**8249–8261.
12. **Goulder, P. J., and B. D. Walker.** 2002. HIV-1 superinfection—a word of caution. N. Engl. J. Med. **347:**756–758.
13. **Grobler, J., C. M. Gray, C. Rademeyer, C. Seoighe, G. Ramjee, S. A. Karim, L. Morris, and C. Williamson.** 2004. Incidence of HIV-1 dual infection and its association with increased viral load set point in a cohort of HIV-1 subtype C-infected female sex workers. J. Infect. Dis. **190:**1355–1359.
14. **Gross, K. L., T. C. Porco, and R. M. Grant.** 2004. HIV-1 superinfection and viral diversity. AIDS **18:**1513–1520.
15. **Harris, M. E., D. Serwadda, N. Sewankambo, B. Kim, G. Kigozi, N. Kiwanuka, J. B. Phillips, F. Wabwire, M. Meehen, T. Lutalo, J. R. Lane, R. Merling, R. Gray, M. Wawer, D. L. Birx, M. L. Robb, and F. E. McCutchan.** 2002. Among 46 near full length HIV type 1 genome sequences from Rakai District, Uganda, subtype D and AD recombinants predominate. AIDS Res. Hum. Retrovir. **18:**1281–1290.
16. **Hoelscher, M., W. E. Dowling, E. Sanders-Buell, J. K. Carr, M. E. Harris, A. Thomschke, M. L. Robb, D. L. Birx, and F. E. McCutchan.** 2002. Detection of HIV-1 subtypes, recombinants, and dual infections in east Africa by a multi-region hybridization assay. AIDS **16:**2055–2064.
17. **Hoelscher, M., B. Kim, L. Maboko, F. Mhalu, F. von Sonnenburg, D. L. Birx, and F. E. McCutchan.** 2001. High proportion of unrelated HIV-1 intersubtype recombinants in the Mbeya region of southwest Tanzania. AIDS **15:** 1461–1470.
18. **Hoffmann, O., B. Zaba, B. Wolff, E. Sanga, L. Maboko, D. Mmbando, F. von Sonnenburg, and M. Hoelscher.** 2004. Methodological lessons from a cohort study of high risk women in Tanzania. Sex. Transm. Infect. **80**(Suppl. 2)**:** ii69–ii73.
19. **Hu, W. S., and H. M. Temin.** 1990. Retroviral recombination and reverse transcription. Science **250:**1227–1233.
20. **Jost, S., M. C. Bernard, L. Kaiser, S. Yerly, B. Hirschel, A. Samri, B. Autran, L. E. Goh, and L. Perrin.** 2002. A patient with HIV-1 superinfection. N. Engl. J. Med. **347:**731–736.
21. **Jung, A., R. Maier, J. P. Vartanian, G. Bocharov, V. Jung, U. Fischer, E. Meese, S. Wain-Hobson, and A. Meyerhans.** 2002. Multiply infected spleen cells in HIV patients. Nature **418:**144.
22. **Kijak, G. H., E. Sanders-Buell, N. D. Wolfe, E. Mpoudi-Ngole, B. Kim, B. Brown, M. L. Robb, D. L. Birx, D. S. Burke, J. K. Carr, and F. E. McCutchan.** 2004. Development and application of a high-throughput HIV type 1 genotyping assay to identify CRF02_AG in West/West Central Africa. AIDS Res. Hum. Retrovir. **20:**521–530.
23. **Koelsch, K. K., D. M. Smith, S. J. Little, C. C. Ignacio, T. R. Macaranas, A. J. Brown, C. J. Petropoulos, D. D. Richman, and J. K. Wong.** 2003. Clade B HIV-1 superinfection with wild-type virus after primary infection with drug-resistant clade B virus. AIDS **17:**F11–F16.
24. **Korber, B. T. (ed.).** 2002. HIV sequence compendium 2002. Theoretical Biology and Biophysics Group, Los Alamos National Laboratory, Los Alamos, N.Mex.
25. **Levy, D. N., G. M. Aldrovandi, O. Kutsch, and G. M. Shaw.** 2004. Dynamics of HIV-1 recombination in its natural target cells. Proc. Natl. Acad. Sci. USA **101:**4204–4209.
26. **Levy, J. A.** 2003. Is HIV superinfection worrisome? Lancet **361:**98–99.
27. **Maciukenas, S.** 1994. Treetool: ribosomal database project. University of Illinois, Urbana-Champagne, Ill.
28. **Mattapallil, J. J., D. C. Douek, B. Hill, Y. Nishimura, M. Martin, and M. Roederer.** 2005. Massive infection and loss of memory CD4+ T cells in multiple tissues during acute SIV infection. Nature **434:**1093–1097.
29. **McCutchan, F. E.** 2000. HIV/AIDS, p. 143–167. *In* R. C. A. Thompson (ed.), Molecular epidemiology of infectious diseases. Edward Arnold Limited, London, United Kingdom.
30. **McCutchan, F. E.** 2000. Understanding the genetic diversity of HIV-1. AIDS **14**(Suppl. 3)**:**S31–S44.
31. **McCutchan, F. E., E. Sanders-Buell, M. O. Salminen, J. K. Carr, and W. H. Sheppard.** 1998. Diversity of the human immunodeficiency virus type 1 envelope glycoprotein in San Francisco men's health study participants. AIDS Res. Hum. Retrovir. **14:**329–337.
32. **Operskalski, E. A., D. O. Stram, M. P. Busch, W. Huang, M. Harris, S. L. Dietrich, E. R. Schiff, E. Donegan, and J. W. Mosley.** 1997. Role of viral load in heterosexual transmission of human immunodeficiency virus type 1 by blood transfusion recipients. Transfusion Safety Study Group. Am. J. Epidemiol. **146:**655–661.
33. **Pedraza, M. A., J. del Romero, F. Roldan, S. Garcia, M. C. Ayerbe, A. R. Noriega, and J. Alcami.** 1999. Heterosexual transmission of HIV-1 is associated with high plasma viral load levels and a positive viral isolation in the infected partner. J. Acquir. Immune Defic. Syndr. **21:**120–125.
34. **Ramos, A., D. J. Hu, L. Nguyen, K. O. Phan, S. Vanichseni, N. Promadej, K. Choopanya, M. Callahan, N. L. Young, J. McNicholl, T. D. Mastro, T. M. Folks, and S. Subbarao.** 2002. Intersubtype human immunodeficiency virus type 1 superinfection following seroconversion to primary infection in two injection drug users. J. Virol. **76:**7444–7452.
35. **Riedner, G., M. Rusizoka, O. Hoffmann, F. Nichombe, E. Lyamuya, D. Mmbando, L. Maboko, P. Hay, J. Todd, R. Hayes, M. Hoelscher, and H. Grosskurth.** 2003. Baseline survey of sexually transmitted infections in a cohort of female bar workers in Mbeya Region, Tanzania. Sex. Transm. Infect. **79:**382–387.
36. **Robertson, D. L., P. M. Sharp, F. E. McCutchan, and B. H. Hahn.** 1995. Recombination in HIV-1. Nature **374:**124–126. (Letter.)
37. **Salminen, M. O., J. K. Carr, D. S. Burke, and F. E. McCutchan.** 1995. Identification of breakpoints in intergenotypic recombinants of HIV type 1 by bootscanning. AIDS Res. Hum. Retrovir. **11:**1423–1425.
38. **Salminen, M. O., C. Koch, E. Sanders-Buell, P. K. Ehrenberg, N. L. Michael, J. K. Carr, D. S. Burke, and F. E. McCutchan.** 1995. Recovery of virtually full-length HIV-1 provirus of diverse subtypes from primary virus cultures using the polymerase chain reaction. Virology **213:**80–86.
39. **Tovanabutra, S., D. L. Birx, and F. E. McCutchan.** 2004. Molecular epidemiology of HIV-1 in Asia and the Pacific, p. 181–205. *In* Y. Lu and M. Essex (ed.), AIDS in Asia. Raven Press, New York, N.Y.
40. **Wain-Hobson, S., C. Renoux-Elbe, J. P. Vartanian, and A. Meyerhans.** 2003. Network analysis of human and simian immunodeficiency virus sequence sets reveals massive recombination resulting in shorter pathways. J. Gen. Virol. **84:**885–895.
41. **Yang, O. O., E. S. Daar, B. D. Jamieson, A. Balamurugan, D. M. Smith, J. A. Pitt, C. J. Petropoulos, D. D. Richman, S. J. Little, and A. J. Brown.** 2005. Human immunodeficiency virus type 1 clade B superinfection: evidence for differential immune containment of distinct clade B strains. J. Virol. **79:**860–868.